

Wakefield generation in metamaterial-loaded waveguides

S. Antipov^{a)} and L. Spentzouris
Illinois Institute of Technology, Chicago, Illinois 60616

W. Liu, W. Gai, and J. G. Power
Argonne National Laboratory, Argonne, Illinois 60439

(Received 23 May 2007; accepted 25 June 2007; published online 14 August 2007)

Metamaterials (MTMs) are artificial structures made of periodic elements and are designed to obtain specific electromagnetic properties. As long as the periodicity and the size of the elements are much smaller than the wavelength of interest, an artificial structure can be assigned a permittivity and permeability, just like natural materials. Metamaterials can be customized to have the permittivity and permeability desired for a particular application. When the permittivity and permeability are made simultaneously negative in some frequency range, the metamaterial is called double-negative or left-handed and has some unusual properties. For example, Cherenkov radiation (CR) in a left-handed metamaterial is backward; radiated energy propagates in the opposite direction to particle velocity. This property can be used to improve the design of particle detectors. Waveguides loaded with metamaterials are of interest because the metamaterials can change the dispersion relation of the waveguide significantly. Slow backward waves, for example, can be produced in a MTM-loaded waveguide without corrugations. In this paper we present theoretical studies of waveguides loaded with an anisotropic and dispersive medium (metamaterial). The dispersion relation of a MTM-loaded waveguide has several interesting frequency bands which are described. We present a universal method to simulate wakefield (CR) generation in a waveguide loaded with a dispersive and anisotropic medium. This method allows simulation of different waveguide cross sections, any transverse beam distribution, and any physical dispersion, of the medium. The method is benchmarked against simple cases, which can be theoretically calculated. Results show excellent agreement. © 2007 American Institute of Physics. [DOI: [10.1063/1.2767640](https://doi.org/10.1063/1.2767640)]

INTRODUCTION

The electromagnetic properties of a medium are characterized by the permittivity ϵ (response to electric field) and the permeability μ (response to magnetic field). Typically ϵ and μ are positive for most frequencies of electromagnetic waves. In this case, the phase vector (k) of the wave forms a right-handed system with the field vectors E and B . The Poynting vector is co-directed with k .

Veselago pointed out that propagation is also possible when ϵ and μ are simultaneously negative.¹ Propagating waves in such double-negative media (DNM) exhibit several unusual properties. First of all, the phase vector forms a left-handed system with the field vectors. This is why materials with simultaneously negative ϵ and μ are called left-handed (LHM). In such media the Poynting vector, which is collinear with the group velocity, is counterdirected to the phase vector. This gives rise to several unusual effects such as the reversed Doppler Effect, reversed Cherenkov radiation (CR),¹⁻⁴ and negative refraction.^{1,5} Cherenkov radiation is widely used in accelerator physics. It has particle detector applications and it may be that reverse Cherenkov radiation is uniquely useful for beam detection.^{3,4,6}

At Argonne Wakefield Accelerator (AWA) Facility we are focused on studies of particle interaction with metamaterials. We have designed and manufactured a double-negative

metamaterial similar to others.⁷ In Refs. 6 and 8 we reported our metamaterial design. We used a known method⁵ to experimentally verify that the refraction of our left-handed metamaterial is negative. We also performed a standard⁹ left-handed transmission measurement for both the configuration of a bulk metamaterial and for a metamaterial-loaded waveguide.¹⁰ We observed much better transmission level and stability to manufacture tolerances for a loaded waveguide. Thus, we are using a metamaterial-loaded waveguide configuration for our further studies.

In this paper, we first discuss the nature of negative permeability and permittivity and how this is reflected in the metamaterial design. We will explain how an artificial permittivity and permeability are produced. Next we present a detailed discussion of the calculation of dispersion relations of TM modes in a rectangular metamaterial-loaded waveguide. The dispersion relations of a loaded waveguide allow a simple way to check whether or not a particular mode will be excited by injected particles moving at speed v , and if so, at what frequency. However, it does not give quantitative results on how much energy each mode will absorb from a particle beam. These values depend on the transverse and longitudinal particle distribution of the beam and scale with the total charge. We present a method to simulate a wakefield generation in a waveguide loaded with an anisotropic and dispersive medium (metamaterial) for any transverse particle distribution. The method is compared with known results for dielectric-loaded accelerators.

^{a)}Electronic mail: antipov@anl.gov

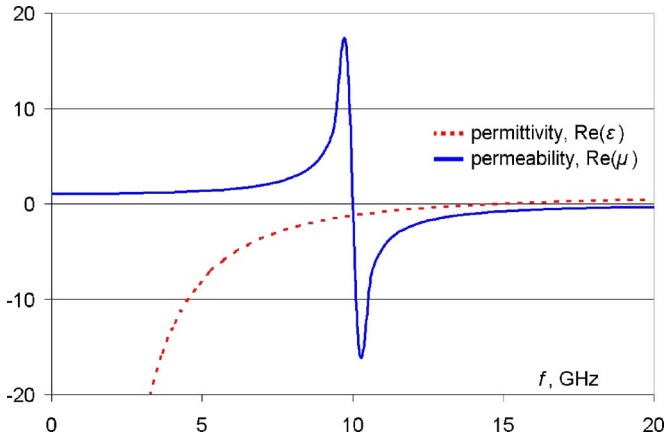


FIG. 1. (Color online) Typical frequency behavior of permittivity and permeability, produced by wire array and array of split ring resonators.

ARTIFICIAL PERMITTIVITY AND PERMEABILITY

Left-handed materials do not exist naturally. LHM was artificially constructed in 2001 (Refs. 5 and 9) using a wire array [which provided $\epsilon < 0$ (Ref. 11)] and an array of split ring resonator (SRR) [which provided $\mu < 0$ (Ref. 12)]. It has been shown¹¹ that a wire array exhibits plasmlike behavior (1) in the gigahertz frequency range (see Fig. 1, dashed line). The frequency dependence of permittivity has the following form:

$$\epsilon(\omega) = 1 - \frac{\omega_p^2}{\omega^2 + i\gamma\omega}, \quad \omega_p^2 = \frac{2\pi c^2}{a^2 \ln(a/r)}$$

$$\text{and } \gamma_e = \frac{c^2}{2\sigma S \ln(a/r)}. \quad (1)$$

Here a is the periodic spacing between wires, r is the wire radius, c is the speed of light and S is the wire cross section. A simple antenna analysis gives the same result.^{13,14} The wire array shown in Fig. 2(a) can produce plasmlike behavior (negative permittivity) only for electric fields that are parallel to the direction of the wires. This structure is anisotropic. In order to have an isotropic tensor, $\epsilon = \epsilon \cdot \hat{I}$, where \hat{I} is the unity matrix, the wires should be assembled in a three-

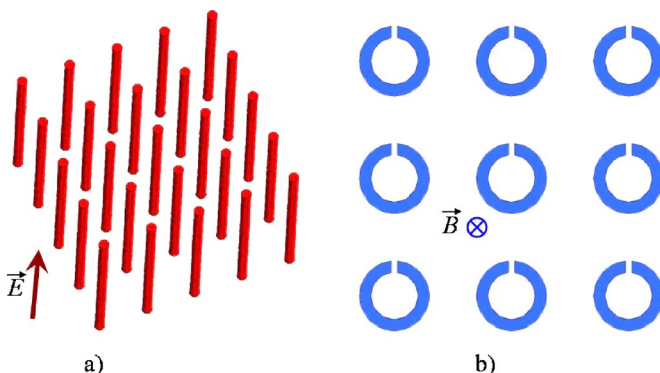


FIG. 2. (Color online) Wire array (a) and array of split ring resonators (b). The structures are anisotropic. An artificial permeability is produced only if magnetic field penetrates through the rings. Plasmlike behavior is observed in the wire array only if electric field polarized along the wires.

dimensional (3D) grid to cover all three possible polarizations of electric field.

In order to realize an artificial μ we turn to magnetic dipoles. A loop of current creates a magnetic dipole. An assembly of small loop structures behaves like a continuous media, provided the radiation wavelength is significantly greater than the geometric scale of the loops. This assembly produces a response to a magnetic field when it penetrates the rings. These rings are usually made thin, so other polarizations of magnetic field do not produce any effect on the rings. This makes metamaterials strongly anisotropic. One has to make an additional effort to make the structure isotropic so that $\mu = \mu \cdot \hat{I}$ by having all three possible orientations of loops \perp to x , y , and z . To create a resonant response one needs to cut the ring [Fig. 2(b)]. The resulting split ring resonator¹² has a distributed self-inductance and a small capacitance in the cut. Therefore the system behaves similarly to an RLC circuit and has a resonance. Our rings have a square form for more efficient space usage. The typical response of such a structure is almost Lorentz-like¹⁵ (see Fig. 1, solid line). The frequency dependence of permeability has the form given by

$$\mu_{\text{eff}} = 1 - \frac{F\omega^2}{\omega^2 - \omega_{\text{res}}^2 + i\gamma\omega}. \quad (2)$$

Here F is a geometrical factor. Constants ω_{res} and γ are also determined by geometry.

The geometry is customized for a particular application. We use two concentric split rings⁷ to increase the capacitive region and lower the resonance frequency. In the design we studied at AWA (Refs. 6 and 8) we had a 2.54 mm overall size of the ring. The resonant frequency was designed and measured at 11.4 GHz ($\lambda \gg d$).

We have measured propagation of the fundamental mode (TE_{10}) in a metamaterial-loaded waveguide. These results are presented in (Ref. 10). We observed much better transmission level and predictability compared to a bulk configuration of metamaterial structure. We have chosen a loaded waveguide configuration for our future metamaterial structure-particle interaction studies. Since we are interested in particle interaction with an electric field along the direction of beam motion, the TM modes in a metamaterial-loaded waveguide will be analyzed.

GENERAL SOLUTION FOR TM AND TE MODES IN A WAVEGUIDE LOADED WITH ANISOTROPIC AND DISPERSIVE MEDIA

The dispersion relation of a waveguide structure can be used to find the frequencies where the phase velocity of a propagating electromagnetic mode in the structure is matched to the velocity of injected particles. Once these synchronous modes are identified, further analysis can be narrowed to a consideration of these particular frequencies.

We will assume a waveguide to be aligned longitudinally with the z axis. A rectangular waveguide is chosen to best match the alignment of the metamaterial. The size of the

waveguide is a along x direction and b along y direction. We chose our metamaterial to have the following tensors for permittivity and permeability.

These properties are realized by the metamaterial design we plan to study experimentally.¹⁰ However, there is an issue of strong spatial dispersion at large wavelengths.¹⁶ We will briefly discuss the consequences of this effect in the Appendix. The following analysis is done for the uniform anisotropic and dispersive medium:

$$\hat{\epsilon} = \begin{pmatrix} \epsilon_{\perp} & 0 & 0 \\ 0 & \epsilon_{\perp} & 0 \\ 0 & 0 & \epsilon_{\parallel} \end{pmatrix}, \quad \hat{\mu} = \begin{pmatrix} \mu_{\perp} & 0 & 0 \\ 0 & \mu_{\perp} & 0 \\ 0 & 0 & \mu_{\parallel} \end{pmatrix}, \quad (3)$$

$$\epsilon_{\perp} = 1 + \frac{\omega_{pe}^2}{\omega_{re}^2 - 2i\omega_{de}\omega - \omega^2}, \quad \epsilon_{\parallel} = 1, \quad (4)$$

$$\mu_{\perp} = 1 + \frac{F\omega^2}{\omega_{rm}^2 - 2i\omega_{dm}\omega - \omega^2}, \quad \mu_{\parallel} = 1, \quad (5)$$

Here ω_{re} , ω_{rm} are resonance frequencies, ω_{pe} is plasma frequency, and ω_{de} , ω_{dm} are attenuation parameters.

In order to find dispersion relations for the modes supported by a loaded waveguide, we start solving Maxwell's equations in the frequency domain, searching for solutions $[\exp(ik_z z)]$ propagating in the z direction. Because of anisotropy we have to write the vector equations separately for each component and simplify the system to get the dispersion relations for the modes. The standard methods of such analysis are described, for example, in Ref. 17 and used for different configurations of metamaterials in. Refs. 18 and 19. We obtain

$$k_z^2 = k_0^2 \epsilon_{\perp} \mu_{\perp} \left(1 - \frac{\chi_x^2 + \chi_y^2}{\epsilon_{\parallel} \mu_{\perp} k_0^2} \right) \quad \text{for TM modes } (k_0 = \omega/c), \quad (6)$$

$$k_z^2 = k_0^2 \epsilon_{\perp} \mu_{\perp} \left(1 - \frac{\chi_x^2 + \chi_y^2}{\epsilon_{\perp} \mu_{\parallel} k_0^2} \right) \quad \text{for TE modes.} \quad (7)$$

Our primary interest is the excitation of metamaterial structures by particles. Since only the TM modes can realize the synchronization condition, we will limit our analysis to TM modes only.

The accelerating structures are usually described by E_z component. The other field components can be expressed in terms of E_z ,

$$H_x = -\frac{ik_0 \epsilon_{\parallel}}{\chi_x^2 + \chi_y^2} \frac{\partial E_z}{\partial y}, \quad H_y = \frac{ik_0 \epsilon_{\parallel}}{\chi_x^2 + \chi_y^2} \frac{\partial E_z}{\partial x}, \quad (8)$$

$$E_x = \frac{\epsilon_{\parallel}}{\epsilon_{\perp}} \frac{ik_z}{\chi_x^2 + \chi_y^2} \frac{\partial E_z}{\partial x}, \quad E_y = -\frac{\epsilon_{\parallel}}{\epsilon_{\perp}} \frac{ik_z}{\chi_x^2 + \chi_y^2} \frac{\partial E_z}{\partial y}.$$

The dispersion relation for TM modes provides several interesting regimes. There are several characteristic frequencies in the ϵ and μ tensors of the medium, which can be adjusted to manipulate the form of the dispersion relation: (1) cutoff frequency of the empty waveguide, (2) plasma frequency for

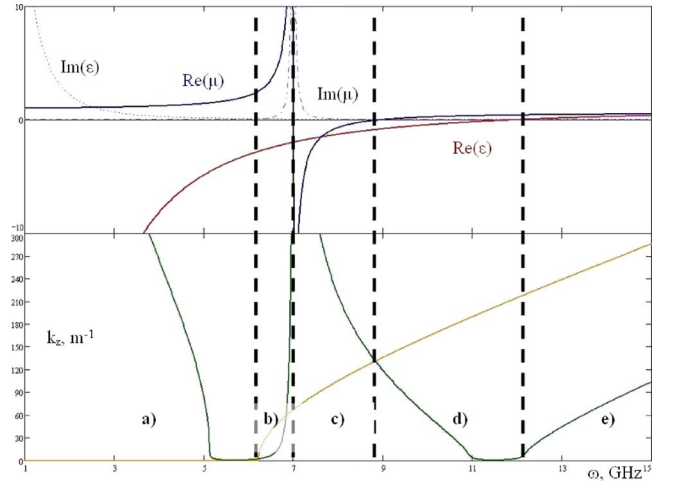


FIG. 3. (Color online) Top: Transverse values of permittivity and permeability. Characteristic frequencies create five frequency domains with different behaviors of the TM mode. Bottom: (green) dispersion of an MTM-loaded waveguide and (orange) dispersion of an empty waveguide. We observe (from left to right) nonmagnetic, $\epsilon < 0$, $\mu > 0$ above cutoff, left-handed, quasi-non-magnetic, and empty-waveguide-like mode regimes.

ϵ_{\parallel} , [Eq. (4)], (3) resonance frequency for μ_{res} [Eq. (5)], and (4) magnetic plasma frequency for μ_{mp} [Eq. (5)].

The typical choice of parameter sequence is $\omega_{cutoff} < \omega_{res} < \omega_{mp} < \omega_p$. This insures we will have a frequency range where ϵ_{\perp} and μ_{\perp} are simultaneously negative. Anisotropic and dispersive media change the dispersion relations for the modes in a waveguide dramatically. The dispersion of an empty waveguide is compared to that of a loaded waveguide in Fig. 3. The transverse ϵ_{\perp} and μ_{\perp} dependence on frequency are plotted above the waveguide dispersion ($\epsilon_{\parallel} = \mu_{\parallel} = 1$) to highlight their effect. The negative slope of the waveguide dispersion corresponds to a backward mode (negative group velocity). There are five different transmission bands in the dispersion of waveguide loaded with anisotropic and dispersive medium, the importance and properties of which are discussed in the Appendix. Here we focus on the range of frequencies most affected by the presence of such medium.

Fast particles (we consider electrons at speed v , close to c) can generate modes in a waveguide loaded with anisotropic and dispersive medium. To show this we plot the electron dispersion ($k_0 = \omega/v$) together with dispersion of the modes. Points where the electron line and mode dispersion intersect indicate the frequencies and phase numbers of modes which can be excited by a particle. However, this method does not give information as to which modes will absorb more energy from the particles. A detailed wakefield (Cherenkov) calculation or simulation is needed (see the next section of this paper).

As can be seen in Fig. 4, in the presence of anisotropy and dispersion for both ϵ and μ , particles can excite various backward modes. There is also a forward regime at the resonant frequency of the permeability (black dot on Fig. 4). However, its group velocity is practically zero, and so we will not consider it further. Figure 5 presents the case when only the permittivity is anisotropic and dispersive ($\mu = 1$). Even in this case there is a possibility of interaction between

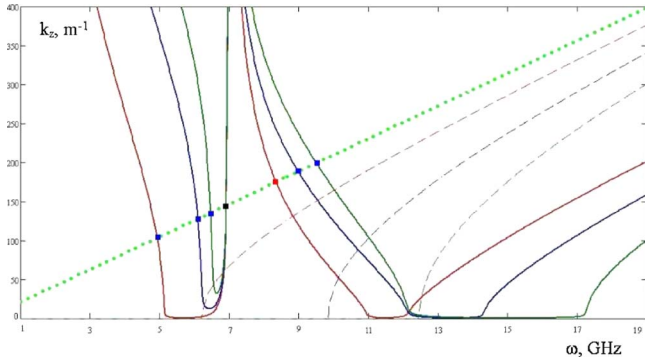


FIG. 4. (Color online) Dispersion of TM_{111} (red), TM_{21} and TM_{12} (blue, degenerate) and TM_{22} (green) modes. Solid lines correspond to LHM-loaded case and dashed lines correspond to empty waveguide. The dotted line is a particle dispersion. There are several different synchronization opportunities in nonmagnetic, left-handed, and quasi-non-magnetic regimes.

particle and a waveguide mode, although it happens below the cutoff frequency for an empty waveguide (see Appendix).

CHERENKOV RADIATION IN A WAVEGUIDE LOADED WITH DISPERSIVE AND ANISOTROPIC MEDIUM

Waveguides loaded with metamaterials can be used for particle detection, particularly as beam diagnostics. In the following section we will consider theoretically some aspects of Cherenkov radiation in waveguides loaded with anisotropic and dispersive media (metamaterial).

The theory of Cherenkov radiation in waveguides with dispersive materials has been discussed in a number of papers (see, for example, Refs. 20–22). Various methods of analysis have been developed for waveguides loaded with both passive^{23–25} and active^{26,27} isotropic materials.

When both dispersion and anisotropy are present the analysis becomes more involved.²⁸ Below we will describe a general method for finding the wakefield of a particle beam traveling through the waveguide loaded with anisotropic and dispersive medium, as well as for finding the power deposited in each mode by the beam. Use of our simulation allows us to skip some of the intermediate steps in the analytic calculation and directly obtain the final result; the excitation spectrum.

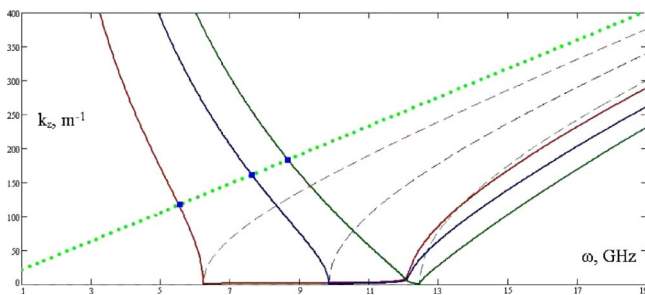


FIG. 5. (Color online) Dispersion of TM_{111} (red), TM_{21} and TM_{12} (blue, degenerate), and TM_{22} (green) modes. Solid lines correspond to ϵ loaded case, $\mu=1$, and dashed lines correspond to empty waveguide. The dotted line is a particle dispersion. The only possibility for particle-mode interaction is in nonmagnetic regime.

We will be solving Maxwell's equations in the frequency domain for the E_z component. Other components of the electric and magnetic fields can be found via the relations given by Eq. (8). For the particle beam source, we assume a narrow longitudinal beam traveling in the z direction at speed v (represented by a delta function), with a transverse particle distribution $T(x, y)$. Sometimes such beam is called a “pancake” beam. The study of beams with finite longitudinal extent can be done once the solution for a pancake beam is known (this provides the needed Green's function). The charge and current density of the beam are given by

$$\rho(\mathbf{r}, t) = \frac{q}{2\pi} \cdot T(x, y) \cdot \delta(z - vt), \quad (9)$$

$$j_z(\mathbf{r}, t) = \frac{q}{2\pi} \cdot v \cdot T(x, y) \cdot \delta(z - vt).$$

The delta functions in Eq. (9) will become $\exp(i \cdot \omega \cdot z/v)$ terms after Fourier transform. Therefore, for the z component of electric field we can also assume the dependence,

$$E_z(x, y, z, \omega) = E_0(x, y) \cdot \exp\left(i \frac{\omega}{v} z\right). \quad (10)$$

Without explicit time and z dependence we obtain a two-dimensional (2D) partial differential equation (PDE) equation for the transverse profile of E_z field $E_0(x, y)$ of the following form:

$$\begin{aligned} -\epsilon_{\perp} \Delta_{\perp} E_0 + \epsilon_{\parallel} \left(\frac{\omega}{v}\right)^2 E_0 - k_0^2 \epsilon_{\parallel} \epsilon_{\perp} \mu_{\perp} E_0 \\ = i \cdot 4\pi \cdot \omega \cdot q \cdot T(x, y) \cdot \left(\frac{\epsilon_{\perp} \mu_{\perp}}{c^2} - \frac{1}{v^2}\right). \end{aligned} \quad (11)$$

Here, the tensors of permittivity and permeability have the form (3). This equation can be simulated in a waveguide cross section. The cross section can be of any form. Zero tangential electric field on the waveguide wall imposes Dirichlet boundary conditions. The dispersion of components of permittivity and permeability can be arbitrary, providing it is physical (satisfies Kramers-Kronig relations).

In principle, Eq. (11) can be solved using a technique based on decomposition of the radiated field into waveguide modes.^{23–27} The transverse beam distribution is decomposed into waveguide cross-section eigenfunctions as well,

$$\begin{aligned} E_0(x, y) &= \sum_i \alpha_i E_{0i}(x, y), \\ T(x, y) &= \sum_i t_i E_{0i}(x, y), \quad \text{with} \end{aligned} \quad (12)$$

$$-\Delta_{\perp} E_{0i} = \lambda_i E_{0i}.$$

Therefore, the solution for Eq. (11) can be obtained in terms of eigenfunctions as

$$E_0(x, y, \omega) = \sum_i \frac{i \cdot (4\pi/\epsilon_{\perp}) \cdot q \cdot \omega \cdot t_i \cdot (\epsilon_{\perp}\mu_{\perp}/c^2 - 1/v^2)}{\lambda_i - (\omega^2\epsilon_{\parallel}/\epsilon_{\perp}) \cdot (\epsilon_{\perp}\mu_{\perp}/c^2 - 1/v^2)} \times E_{0i}(x, y). \quad (13)$$

Transforming back to the time domain brings us to a solution in a general form as an integral of a sum with singularities in the denominator,

$$E_z(x, y, z, t) = \sum_i 4\pi i \cdot q t_i E_{0i}(x, y) \times \int_{-\infty}^{+\infty} \frac{\omega/\epsilon_{\perp} (\epsilon_{\perp}\mu_{\perp}/c^2 - 1/v^2) \cdot e^{i\omega(z/v-t)}}{\lambda_i - (\omega^2\epsilon_{\parallel}/\epsilon_{\perp}) \cdot (\epsilon_{\perp}\mu_{\perp}/c^2 - 1/v^2)} d\omega. \quad (14)$$

The theory of residues is used to evaluate the integral. The poles of the function under integration lie on the integration path. This makes the solution nonunique. The values of the integral for the route passing over the poles and passing under the poles both satisfy Maxwell equations. We need to use the causality principle to determine which solution is physical.

For simple cases of anisotropy and dispersion it is possible to take the integral (14) analytically. In the case of dispersive and anisotropic content of the waveguide the integral is harder to analyze. Typical examples of such analysis can be found.^{27,28}

SIMULATION OF WAKEFIELD GENERATION IN A WAVEGUIDE LOADED WITH DISPERSIVE AND ANISOTROPIC MEDIUM

A PDE simulation provides the result without the complete theoretical analysis, making it possible to analyze various cross sections of the waveguides, different transverse charge distributions, and more complicated cases of dispersion including anisotropy and losses. Simulation provides the excitation spectrum and a time-dependent wakefield behind the charge.

We pick the finite element method (FEM) to simulate PDE (11) of wakefield generation because of its flexibility in terms of meshing subdomains. A very fine mesh may be applied to resolve a physically small beam, when its cross section $T(x, y)$ is much smaller than a waveguide aperture. We simulate Eq. (11) parametrically, with parameter ω , for any transverse beam distribution $T(x, y)$. The result of a simulation is the whole sum (13), which is a function of frequency. We observe the regions where this sum diverges (Fig. 6). These regions correspond to the poles of the integral (when denominator is zero) (14).

One way to postprocess the results of a simulation is to take the Fourier transform and obtain the wakefield as a function of time behind the particle. Values near the frequencies where the sum diverges must be properly resolved in simulation. Figure 7 shows the Fourier transform of a simulation result giving the wakefield of a particle distribution moving through a loaded waveguide.

In order to check our method, we simulated a cylindrical waveguide loaded with an isotropic dielectric with a negligibly small beam channel. This case has been discussed in

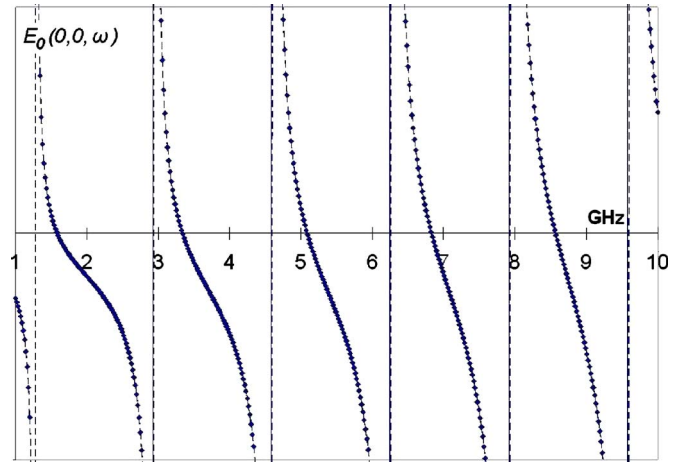


FIG. 6. (Color online) Simulation results for $E_0(0,0,\omega)$. We can see that the result diverges at frequencies corresponding to the mode excitation.

several papers,^{21,29–31} mostly in connection to a dielectric-loaded accelerator (DLA). We compared our simulation results with scripts based on exact solutions.^{30,31} Results show excellent agreement, as seen in Figs. 7 and 8.

Another way to analyze the wakefield is to plot the spectrum of modes. The relative amplitudes of the modes show which modes absorb more energy from the particle. To obtain this plot from the simulation results we have to take a closer look at the dispersion relations and the integral (14). As we can see in the case of dispersion (Figs. 3–5) all the poles of the integral are of the first order. Higher order poles would correspond to the electron dispersion having the same first derivatives as the mode dispersion in the points of intersection on Figs. 4 and 5. This condition is hard to realize theoretically and is practically impossible to create with metamaterials due to manufacturing tolerances. Each divergence of E_0 as a function of ω is treated as a first-order pole

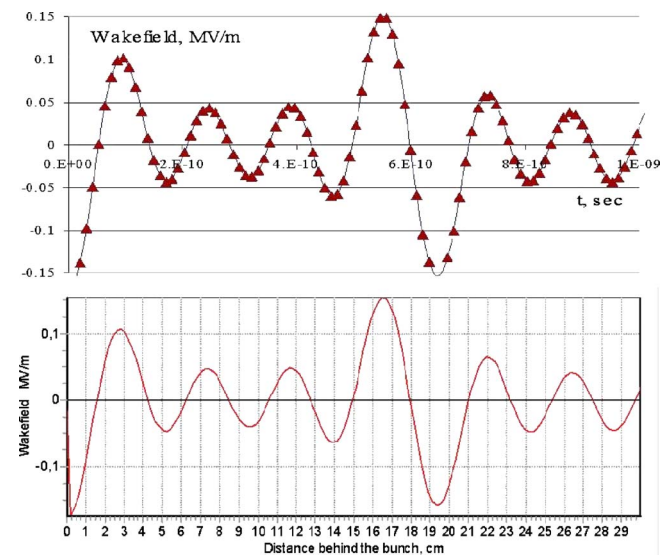


FIG. 7. (Color online) Results for a cylindrical waveguide ($r=3$ cm) loaded with isotropic dielectric ($\epsilon=10$). Top: Fourier transform of the simulation result, wakefield behind the 1 nC bunch, considering first 6 modes. Bottom: Same result from dielectric-loaded accelerator code, based on Ref. 31. Time scale corresponds to a length scale through $l=v^*t$. For particle under consideration $v=0.99c$.

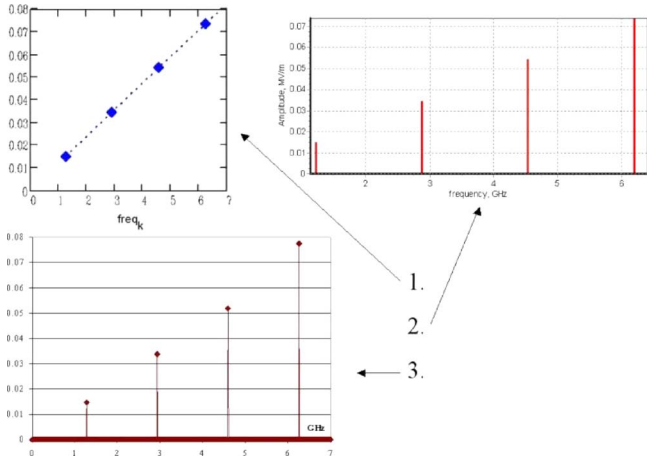


FIG. 8. (Color online) Results for a cylindrical waveguide ($r=3$ cm) loaded with isotropic dielectric ($\epsilon=10$). (1) Results from a script, based on. Ref. 30. (2) Same result based on. Ref. 31. (3) Results from FEM simulation.

on the complex plane of the integral (14). The value of the residue of a first-order pole can be obtained: $\text{Res}(f, z=z_0) = \lim_{z \rightarrow z_0} (f(z) \cdot (z - z_0))$. Therefore we get rid of the divergence by multiplying the simulation results by proper $(\omega - \omega_0) \cdot f(\omega_0)$ values. This provides us with the correct amplitudes for each of the excited modes. We compare our simulation results with theoretical results for the case of a cylindrical waveguide loaded with isotropic nondispersive dielectric. We see good agreement between the simulation and the exact solution (Fig. 8).

For the next example we will consider the anisotropic and dispersive medium used for the dispersion curve analysis (Figs. 3 and 4). We use the transverse particle distribution shown in Fig. 9, representing a 1 nC, 1 μm full width at half maximum (FWHM) size beam, passing off center through the waveguide. We plot it on a grid to show that the mesh is locally enhanced at the center of the transverse beam distribution. The results are shown in Fig. 10. We plot the spectrum of the E_x component of the electric field, measured on the wall of the waveguide, as is planned for the experiment. We observe the excitation of a discrete set of frequencies.

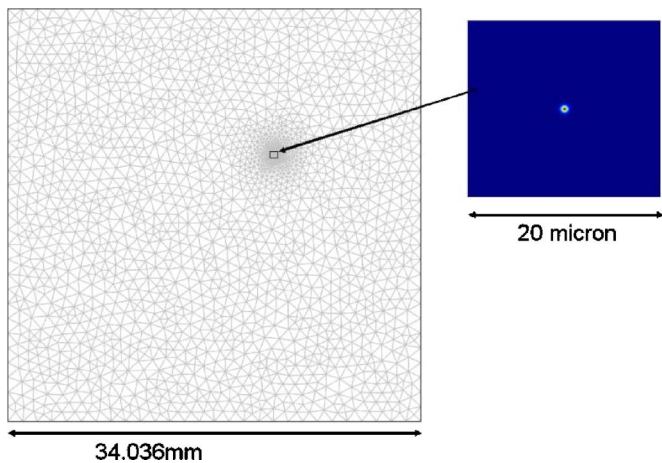


FIG. 9. (Color online) Irregular mesh in finite element method. Mesh is refined in the center to resolve a micron size off-centered beam with 1 nC charge passing through the waveguide.

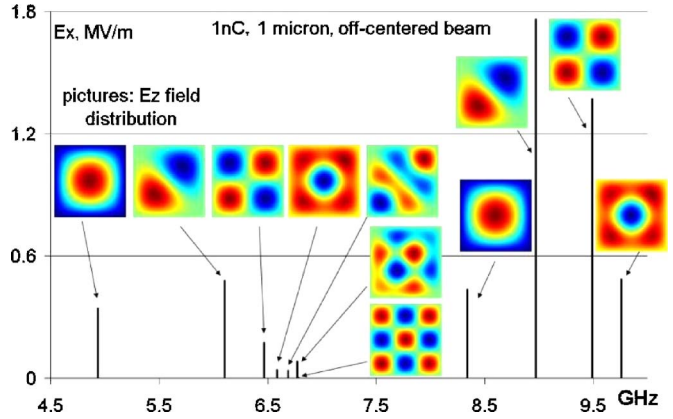


FIG. 10. (Color online) E_x , MV/m on the sidewall of the waveguide, spectrum. Pictures show the field distribution at particular value of a parameter ω .

The delta-function peaks correspond perfectly to the intersections between the dispersion curves and the electron line in Fig. 4. Once we plot the $E_0(x, y)$ field distribution at the excited frequencies, we see that each frequency corresponds to a particular mode. Some modes such as TM_{12} and TM_{21} are degenerate, and we observe a linear combination of these modes at the excitation frequencies. The relative amplitudes of the TM_{12} and TM_{21} modes depend on the transverse particle distribution. Figure 10 shows that for a misaligned beam there is excitation of a linear combination of TM_{12} and TM_{21} . Close to 6.5 GHz we observe a linear combination of TM_{13} and TM_{31} , then TM_{32} and TM_{23} , followed by TM_{14} and TM_{41} .

If the beam is placed in the center of the waveguide we see that the modes absorb energy from the beam differently than in the previous case of a misaligned beam. Dipole modes are not excited (Fig. 11).

SUMMARY

We investigated the interaction of a charged particle distribution with dispersive anisotropic medium (metamaterials). This was done using a uniform media approximation, where an effective medium substitutes for the metamaterial it

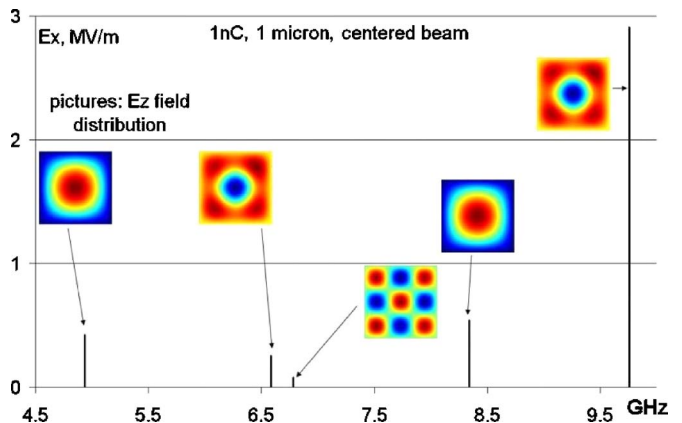


FIG. 11. (Color online) Beam passing through the center of the waveguide. E_x , MV/m on the sidewall of the waveguide spectrum. Pictures show the field distribution at particular frequency ω . Dipole modes are not excited because of symmetry.

is supposed to mimic. However, wire array-based metamaterial unlike a uniform medium has a strong spatial dispersion at large wavelengths.¹⁶ This effect is briefly discussed in the Appendix. The effective medium has the appropriate tensors of permittivity and permeability to match the character of the metamaterial. The particular case of two-axis crystal was studied, since this closely matches the realization of our metamaterial. We used calculated dispersion curves to analyze the particle interaction with the modes of metamaterial-loaded waveguide. This method is simple and provides the frequencies of the modes which can be excited by the particle traveling through such system at speed v . However, it does not tell which mode will absorb more energy from the particle. This depends on the transverse and longitudinal beam distribution and linearly scales with the total charge. A simulation approach is described that treats the problem of a beam propagating through the waveguide loaded with an anisotropic and dispersive medium. The method also allows us to study various waveguide cross sections and transverse beam distributions. We checked the simulation against known codes for dielectric-loaded accelerators based on exact solutions. Then we presented results for wakefield generation in the waveguide loaded with anisotropic and dispersive media. Single particle representation in a simulation is discussed. The finite element method makes it possible to simulate physically small (much smaller than the waveguide cross section) sources due to the possibility of refining the mesh locally at the places of interest.

Waveguides loaded with anisotropic and dispersive media have various interesting regimes of TM-mode propagation and excitation. We show three types of backward modes: non-magnetic, left-handed, and quasinonmagnetic. Such systems may be of interest for particle detection. Metamaterial-loaded waveguides may be used, for example, as beam-position monitors³² and multithreshold detectors.

ACKNOWLEDGMENTS

We are very grateful to Porter W. Johnson, Andrey V. Tyukhtin, and Alexei D. Kanareykin for fruitful discussions. This work is partially supported by the US DOE, Division of High Energy Physics, under Contract No. DE-AC02-06CH11357 and National Science Foundation Grant No. 0237162.

APPENDIX: METAMATERIAL-LOADED WAVEGUIDE OPERATION REGIMES

Previously we reported our derivation of a dispersion relation for a waveguide loaded with anisotropic and dispersive media. Here we limit ourselves to analysis of TM modes in such waveguides; these are the modes of interest for particle beam applications. Figure 3 shows the significant difference in the dispersion of an empty and metamaterial-loaded waveguide. Characteristic frequencies of the system, such as the cutoff frequency of the empty waveguide and frequencies at which ε_{\perp} or μ_{\perp} change their sign, create five different frequency bands for TM mode propagation in a metamaterial-loaded waveguide. In Fig. 3 these bands are denoted by letters and separated by vertical dashed lines.

(a) $\varepsilon < 0$ and $\mu > 0$. This is the nonmagnetic band similar

to the one discussed in Refs. 18, 33, and 34. We see (region I, Fig. 3) the propagation of the mode (real k_z) below the cutoff frequency, similar to Ref. 35 (non- ε). There is a small nonpropagating region due to large values of μ . It is not very interesting and we do not discuss it further.

- (b) $\varepsilon > 0$ and $\mu > 0$. There is no propagation in this region according to Eq. (6).
- (c) $\varepsilon > 0$ and $\mu > 0$. In this region we observe classical left-handed behavior. The resonant behavior of negative μ [Eq. (5)] causes the dispersion curve of the loaded waveguide to intersect with the dispersion of highly relativistic electrons ($\omega = k \cdot c$) (Fig. 4). Therefore an interaction between the electrons and the backward mode is possible, allowing energy exchange.
- (d) $\varepsilon > 0$ and $1 > \mu > 0$. Nevertheless, propagation is possible, because low values of μ make an effective cutoff frequency ($\omega_{\text{cutoff}}^2 / \mu$) higher than the frequency in this band. This band does not require negative values of μ to create a backward propagating mode. This quasi-non-magnetic band requires the condition $1 > \mu > 0$ which can be realized by natural diamagnetics. Further, once $\mu > 1$ propagation vanishes. This region is not very interesting and we do not study it further.
- (e) $\varepsilon > 0$ and $\mu > 0$. The behavior of the system resembles the behavior of an empty waveguide. There is no interaction between the relativistic electrons and the mode.

These bands are important for future metamaterial development. The idea of using a waveguide as an effective media has been discussed in several papers.^{18,19,33–36} It was emphasized that anisotropy plays a great role in realization of non-magnetic regime. The nonmagnetic regime is attractive because it does not require split ring resonators. A split ring resonator has a relatively high imaginary part for permeability (loss) at the resonance. It is also very difficult to scale it to terahertz and optical frequencies.^{18,33,34} The nonmagnetic regime may allow us to create a left-handed metamaterial without the split rings.

We had some discussion on the feasibility of realizing left-handed behavior in the nonmagnetic regime, by loading a wire array into a waveguide in. Ref. 36. Operation below the cutoff frequency of an empty waveguide loaded with the wire array is similar to a problem of wire array embedded into a uniform medium with negative permeability, discussed in. Ref. 37. It has been shown that such system does not support transmission. Another way to explain this phenomenon is to note that wire array exhibits a strong spatial dispersion even in large wavelength limit.¹⁶ It has been shown that metamaterial based on the wire array does not support nonmagnetic band. However, nonmagnetic band can be realized with natural anisotropic materials such as liquid helium cooled bismuth.³³ The quasi-non-magnetic regime may offer another alternative, since it is above the cutoff frequency of an empty waveguide.

If we go back to dispersion plots done for a continuous medium (Figs. 4 and 5), we see that there are nonmagnetic excitations—excitation of a mode by a particle in a nonmagnetic regime (blue points). All higher order modes synchro-

nize in nonmagnetic band. Secondly, for some modes there is synchronization with particles in a left-handed regime (red point), which is our current interest. Finally it is possible to generate modes in quasi-non-magnetic regime (for slightly different medium parameters red point could be in there). Based on the fact that nonmagnetic band does not exist for the wire array configurations, we proposed a system which does not support higher order mode synchronization.³⁶

- ¹V. G. Veselago, *Sov. Phys. Usp.* **10**, 509 (1968).
- ²V. E. Pafomov, *Sov. Phys. JETP* **9**, 1321 (1959).
- ³J. Lu, T. M. Grzegorzczak, Y. Zhang, J. Pacheco, B. I. Wu, J. A. Kong, and M. Chen, *Opt. Express* **11**, 723 (2003).
- ⁴Yu. O. Averkov and V. M. Yakovenko, *Phys. Rev. B* **72**, 205110 (2005).
- ⁵R. Shelby, D. R. Smith, and S. Schultz, *Science* **292**, 77 (2001).
- ⁶S. Antipov, W. Liu, J. Power, and L. Spentzouris, *IEEE Proc. PAC 2005*, pp. 458–460.
- ⁷R. W. Ziolkowski, *IEEE Trans. Antennas Propag.* **51**, 7 (2003).
- ⁸S. Antipov, W. Liu, J. Power, and L. Spentzouris (<http://www.hep.anl.gov/awa/wfnotes/wf229.pdf>).
- ⁹R. A. Shelby, D. R. Smith, S. C. Nemat-Nasser, and S. Schultz, *Appl. Phys. Lett.* **78**, 4 (2001).
- ¹⁰S. Antipov, W. Liu, W. Gai, J. Power, and L. Spentzouris, *Nucl. Instrum. Methods Phys. Res. A* (to be published).
- ¹¹J. B. Pendry, A. J. Holden, W. J. Stewart, and I. Youngs, *Phys. Rev. Lett.* **76**, 4773 (1996).
- ¹²J. B. Pendry, A. J. Holden, D. J. Robbins, and W. J. Stewart, *IEEE Trans. Microwave Theory Tech.* **47**, 2075 (1999).
- ¹³A. A. Zharov, I. V. Shadrivov, and Y. S. Kivshar, *Phys. Rev. Lett.* **91**, 037401 (2003).
- ¹⁴W. Rothman, *IRE Trans. Antennas Propag.* **AP-9**, 82 (1962).
- ¹⁵B. K. P. Scaife, *Principles of Dielectrics*, 2nd ed. (Clarendon, Oxford, 1998).
- ¹⁶P. A. Belov, R. Marques, S. I. Maslovski, I. S. Nefedov, M. Silveirinha, C. R. Simovski, and S. A. Tretyakov, *Phys. Rev. B* **67**, 113103 (2003).
- ¹⁷L. D. Landau, E. M. Lifshitz, and L. P. Pitaevskii, *Electrodynamics of Continuous Media*, 2nd ed. (Butterworth, Oxford, England, 1984).
- ¹⁸V. A. Podolskiy and E. E. Narimanov, *Phys. Rev. B* **71**, 201101(R) (2005).
- ¹⁹I. G. Kondrat'ev and A. I. Smirnov, *Phys. Rev. Lett.* **91**, 249401 (2003).
- ²⁰V. P. Zrelov, *Cherenkov Radiation in High-Energy Physics* (Israel Program for Scientific Translations, Jerusalem, 1970).
- ²¹B. M. Bolotovskiy, *Usp. Fiz. Nauk* **75**, 295 (1961).
- ²²L. Schächter, *Phys. Rev. E* **62**, 1252 (2000).
- ²³A. V. Tyukhtin, *Tech. Phys. Lett.* **30**, 605 (2004).
- ²⁴A. V. Tyukhtin, *Tech. Phys. Lett.* **31**, 150 (2005).
- ²⁵A. D. Kanareykin, and A. V. Tyukhtin, *Nucl. Instrum. Methods Phys. Res. A* **558**, 62 (2006).
- ²⁶N. V. Ivanov and A. V. Tyukhtin, *Tech. Phys. Lett.* **32**, 449 (2006).
- ²⁷A. V. Tyukhtin, A. D. Kanareykin, and P. Schoessow, *AIP Conf. Proc.* **877**, 468 (2006).
- ²⁸A. V. Tyukhtin, S. Antipov, A. D. Kanareykin, and P. Schoessow, *IEEE Proc. PAC 2007* (to be published).
- ²⁹L. Schächter, *Beam-Wave Interaction in Periodic and Quasi-Periodic Structures* (Springer-Verlag, Berlin, 1997), Chap. 4, pp. 157–160.
- ³⁰M. Rosing and W. Gai, *Phys. Rev. D* **42**, 1829 (1990).
- ³¹A. Kanareykin, I. Sheinman, and A. Altmark, *Tech. Phys. Lett.* **28**, 916 (2002).
- ³²S. Banna, L. Ludwig, and L. Schächter, *Nucl. Instrum. Methods Phys. Res. A* **555**, 101 (2005).
- ³³V. A. Podolskiy, L. Alekseyev, and E. E. Narimanov, *J. Mod. Opt.* **52**, 2343 (2005).
- ³⁴R. Wangberg, J. Elser, E. E. Narimanov, and V. Podolskiy, *J. Opt. Soc. Am. B* **23**, 498 (2006).
- ³⁵R. Marqués, J. Martel, F. Mesa, and F. Medina, *Phys. Rev. Lett.* **89**, 183901 (2002).
- ³⁶S. Antipov, W. Liu, W. Gai, J. Power, and L. Spentzouris, *AIP Conf. Proc.* **877**, 815 (2006).
- ³⁷A. L. Pokrovsky and A. L. Efros, *Phys. Rev. Lett.* **89**, 093901 (2002).